# Effect of Intense Plastic Straining and Subsequent Heat Treatment on Mechanical Properties of an Al-Li-Mg-Sc-Zr Alloy

Anna Mogucheva , Rustam Kaibyshev

**Keywords:** Severe plastic deformation; Aluminum-lithium alloy; Precipitations; Microstructures; Mechanical properties

**Abstract.** An Al-5.1%Mg-2.1%Li-0.17%Sc-0.08%Zr (in mass%) alloy designated as 1421 Al was subjected to equal channel angular extrusion (ECAE) with rectangular shape of channels up to fixed true strains of ~4 and ~8 at a temperature of 325°C. This processing provided the formation of uniform recrystallized structures with micron scale average grain size. The 1421 Al after ECAE processing and in initial hot extruded condition was subjected to solution treatment followed by oil quenching and subsequent ageing. Fine grained structure evolved under ECAE remains essentially unchanged under solution treatment. However, this structure affects significantly the precipitation sequence during ageing. Relationships between microstructure and service mechanical properties are considered.

## Introduction

Enhancement of service properties of Al-Li-Mg alloys is very important for their commercial applications as structural materials in aerospace industry [1]. Extensive grain refinement through ECAE is very attractive because of the potential to obtain significant increment in strength of these alloys. The Hall–Petch equation states that the yield stress, $\sigma_y$, is given by

$$\sigma_y = \sigma_0 + k_y \times d^{-1/2} \quad (1),$$

where $\sigma_0$ and $k_y$ are constants determined experimentally. A reduction in the grain size leads to an increase in strength. However, the grain size plays an important but not a dominant role in strength of precipitation-hardened aluminum alloys. Merely achieving micron scale grain size is not sufficient to enhance service properties. Strength of these alloys is significantly increased by dispersion strengthening [2]. Only combination of grain refinement strengthening and precipitation strengthening can provide an increase in strength of Al-Li-Mg alloys.

In addition, these alloys are hard to be deformed at temperatures lower than 250°C due to insufficient ductility. As a result, these alloys can be subjected to ECAE in the temperature interval 300-400°C to produce commercial scale rods or plates with ultrafine grained (UFG) structure [3-6]. Therefore, in order to fabricate Al-Li-Mg alloys with extremely small grain sizes being beneficial in viewpoint of enhancement of their strength under exploitation conditions a post-ECAE heat treatment consisting of solution treatment followed by quenching and subsequent artificial or natural ageing has to be applied. However, the post-ECAE solution treatment can lead to significant grain growth in Al-Li alloys and, therefore, no significant increment in strength of Al-Li alloys processed by ECAE takes place [7, 8]. For instance the strength of ECAE processed Weldalite alloys was found to be lower after T4 treatment and higher after T6 treatment in comparison with these alloys subjected to conventional extrusion [8]. In the same time the combination of ECAE with subsequent heat treatment resulted in increased ductility [8].

In this study the feasibility to use ECAE to enhance service properties of the 1421 Al is evaluated. It was shown previously that ECAE at 325°C provided the formation of UFG structure [3, 6]. ECAE processing can give a positive effect on the mechanical properties of the 1421 Al if UFG structure will be stable under solution treatment and ageing will provide significant strengthening. Therefore, the aim of present study is twofold: (i) consideration of microstructural

evolution of UFG structure under solution treatment; (ii) examination of effect of heat treatment on mechanical properties and phase composition of the 1421 Al.

## Experimental material and procedures

The experiments were carried out using the 1421 Al with a chemical composition of Al-5.1%Mg-2.1%Li-0.17%Sc-0.08%Zr (weight pct). The 1421 Al was manufactured by direct chill casting followed by solution treatment at 425°C for 12 hours. The ingot was initially extruded in the temperature interval 360-390°C with a reduction of 60pct. Details of ECAE using a die with a rectangular cross-section of 125 x 25 $mm^2$ and a height of 125 mm were reported in work [6]. The plates machined from the extruded ingot were pressed 4 and 8 times through the ECAE die at a temperature of 325°C with approximate total accumulated strains of ~4 and ~8. The samples strained up to e~4 were rotated by 90° around the Z axis between each pass in the same direction. In addition, the samples were rotated by 180° around the X axis (Fig.1), i.e. the modified route $B_{CZ}$ [6, 9, 10] was used. The samples strained up to e~8 were rotated by 180° around the X-axis, i.e. route $C_x$ was used [10]. The pressing speed was approximately 3 mm/s. After ECAE the plates were subjected to heat treatment including solution treatment at 450°C for 2h., quenching in oil followed by aging at 120°C for 6 hours.

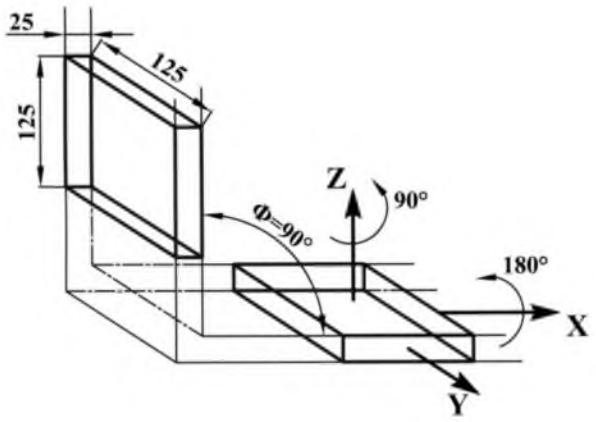


Fig.1. Schematic illustration of rectangular plate for ECAE.

The methods of optical metallography (OM), transmission electron microscopy (TEM), cavitation studies and electron backscattering diffraction (EBSD) analysis were described in previous papers [3, 4, 6]. Terms 'grain' and 'subgrains' are used for definition of crystallites, which are entirely delimited by high angle boundaries (HAGBs) and low angle boundaries (LAGBs), respectively [11]. The '(sub)grains' are crystallite which are bounded partly by LAGBs and partly by HAGBs [11]. Thin foils were examined using a Jeol-2100 TEM with a double-tilt stage and equipped with energy dispersive spectrum analysis (EDS) produced by Oxford Instruments, Ltd at an accelerating potential of 200 kV.

Tensile specimens of 6 mm gauge length and 1.4 x 3 $mm^2$ cross-section were machined from the plates 62x20x100 $mm^3$ with tension axis lying parallel to direction of last extrusion. These samples were tensioned to failure at ambient temperature and a strain rate of 5.6 x $10^{-3}$ $s^{-1}$ using an Instron 5882 testing machine.

## Experimental results

**Microstructure after extrusion.** The microstructure of the 1421 Al subjected to hot extrusion followed by the T6 heat treatment consists of coarse grains elongated toward extrusion axis with dimensions in longitudinal and transverse directions of 171 μm and 21 μm, respectively (Fig.1 from [6]). Chains of recrystallized grains with equiaxed shape and an average size of ~5μm are located

along separate initial grain boundaries. Well-defined subgrain structure was observed within highly elongated grains (Fig.2a). The density of lattice dislocations within (sub)grains ($\rho$~4.5x$10^{13}$ $m^{-2}$ ) is not high. Volume fraction of the $S_1$-phase does not exceed 2pct; particles of $S_1$-phase ($Al_2LiMg$) with average size ranging from 0.5 to 0.7μm exhibit equiaxed shape (Fig.2a). These particles are predominantly located on HAGBs or LAGBs. In addition, coarse particles of S"-phase with an average size ranging from 2 to 4 μm comprise chains located along extrusion axis. A uniform distribution of very fine δ'– particles within grain interiors were found (Fig.2b). These disperoids have an average size of ~5 nm and coherent interface boundaries.

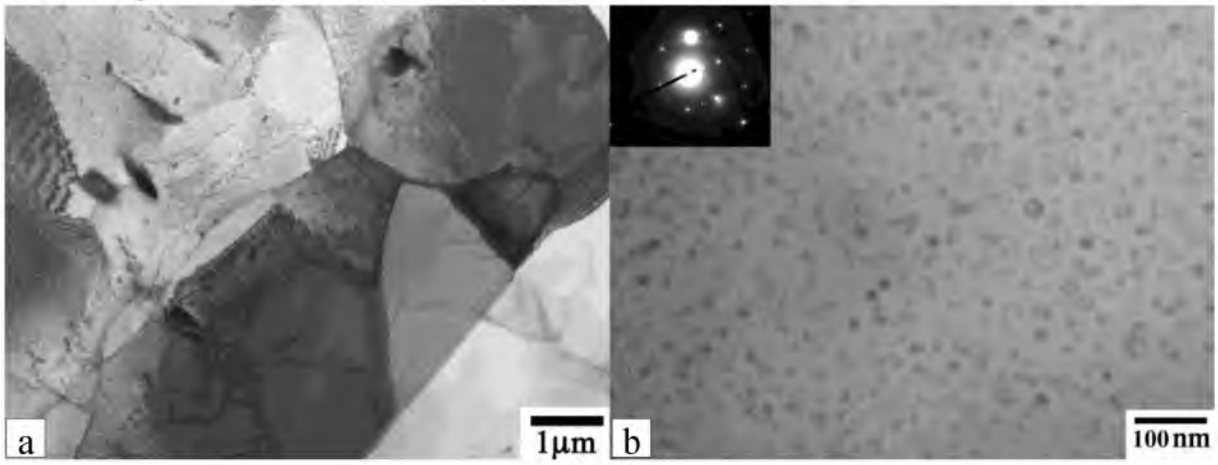


Fig. 2. Typical microstructures of the 1421Al after hot extrusion followed by the T6 heat treatment.

**Microstructure after $\varepsilon$~4.** Uniform recrystallized structure evolved under ECAE with $\varepsilon$~4 (Fig.3a). Population of HABs is ~82 pct; the average misorientation is 34.5°. The fraction of recrystallized grains with an average size of ~1 μm is very high ~95 pct. Microstructural evolution under conditions of solution treatment is characterized by two different types of grain growth process (Fig.3b). Continuous grain growth resulting in minor increase in an average grain size up to ~2 μm is dominated. As a result, relatively high density of lattice dislocations ($\rho$~5x$10^{14}$ $m^{-2}$) remains after the T6 treatment. Large areas of recrystallized grains alternate with coarse bands surrounded by HAGBs. The formation of these bands associates with discontinuous grain growth. The formation of this second structural component leads to a decrease in volume fraction of grains (~81pct.); population of HAGBs (~80pct) and average misorientation (~30.7°). It is seen that the solution treatment have a moderate effect on the recrystallized structure. In contrast, the deformed structure strongly influences the precipitation sequence during ageing. Particles of $S_1$-phase with an average size of 0.4 μm were found at HAGBs and even within grain interiors (Fig.3c). Their volume fraction attends ~16 pct. There is a weak evidence for the formation of the δ' – phase dispersoids (Fig.3d); their volume fraction is negligible.

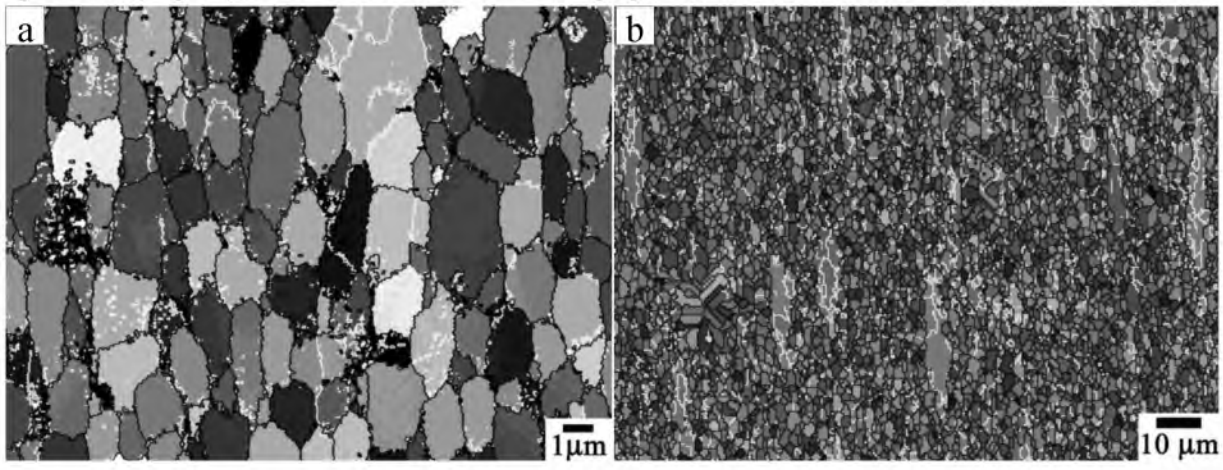

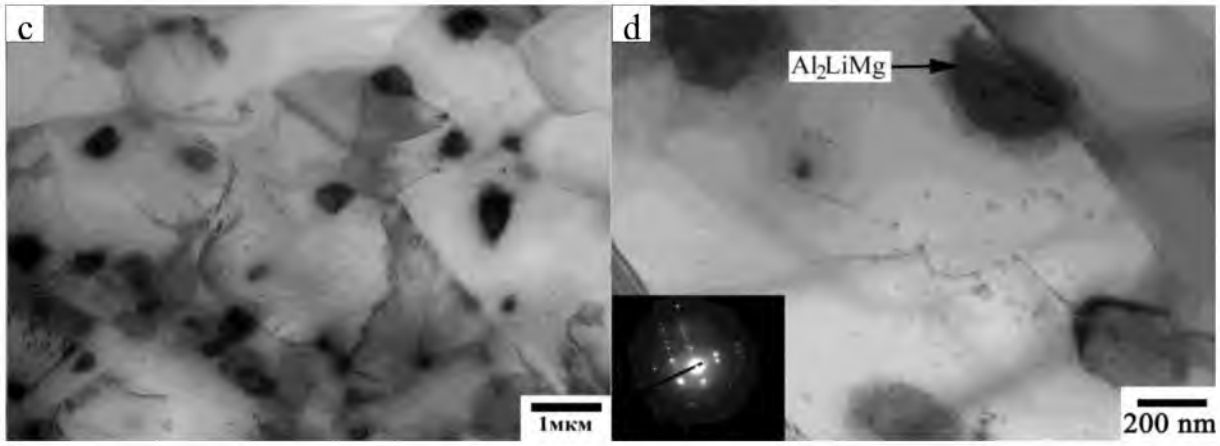


Fig. 3. Typical microstructures of the 1421Al subjected to ECAE with $\varepsilon$~4: (a) after ECAE, (b-d) after ECAE followed by the T6 heat treatment.

**Microstructure after $\varepsilon$~8.** The uniformity of recrystallized structure increases with strain (Fig.4a). Areas of grains with an average size of ~2 μm and (sub)grains with an average size of ~2.3 μm alternate with areas of subgrains. Portion of HAGBs is ~81pct; average misorientaion is 34.5°. As a result, discontinuous grain growth under solution treatment is hindered, significantly (Fig.4b); the volume fraction of coarse elongated grains is less than 10 pct after the T6 heat treatment. Dimensions of grains, (sub)grains and grains, lattice dislocation density after solution treatment following ECAE with $\varepsilon$~4 and $\varepsilon$~8 are essentially the same. The volume fraction of grains is about 85 pct; the population of HABs is ~72 pct., average misorientation (~30.7°). High volume fraction of $S_1$-phase particles (~18pct) was observed after the T6 heat treatment (Fig.4c). No evidence for precipitations of δ'-phase was found (Fig.4d).

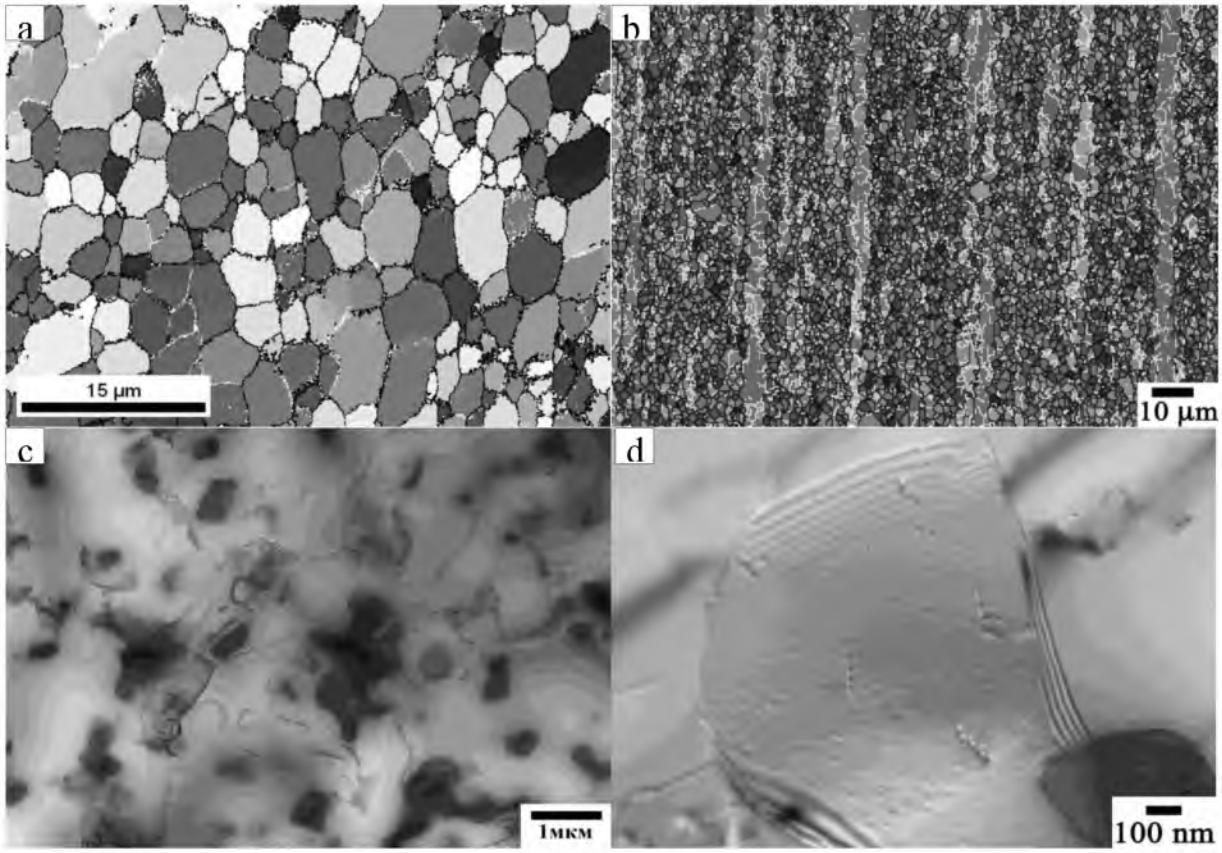


Fig. 4. Typical microstructures of the 1421Al subjected to ECAE with $\varepsilon$~8: (a) after ECAE, (b-d) after ECAE followed by the T6 heat treatment.

**Mechanical properties**. The engineering stress-strain curves of the 1421 Al are shown in Fig.5. The yield stress, ultimate strength and total elongation are summarized in Table 1.

Table 1. Mechanical properties of the 1421 Al alloy at room temperature after the T6 heat treatment

| State of the 1421 Al | $\sigma_{0.2}$, MPa | $\sigma_B$, MPa | $\delta$, % |
|---|---|---|---|
| As-received | 400 | 522 | 14.3 |
| 4 pass ECAE | 371 | 483 | 13.1 |
| 8 pass ECAE | 314 | 398 | 15 |

It is seen that shape of the $\sigma$-$\varepsilon$ curves after ECAE and conventional extrusion, both of which were subjected to subsequent the T6 heat treatment, is similar. Extensive strain hardening takes place after reaching a yield stress. As a result, uniform elongation occurs up to failure providing total elongation higher than 10% for all samples subjected to ECAE with different strains. It is worth noting that this type of the $\sigma$-$\varepsilon$ curves is attributed to materials with micron scale grain size having moderate dislocation density. The values of ductility obtained can be considered as sufficient [2] for Al-Li-Mg alloys. It is possible to conclude that T6 heat treatment following ECAE provides moderate ductility associated with significant strain hardening. In the same it possible to say that ECAE results in decreased yield stress and ultimate strength in comparison with conventional extrusion. It is worth noting that yield stress and ultimate strength of the samples subjected to ECAE with a total strain of ~4 is higher than that for the samples subjected to ECAE with a total strain of ~8 (Table 1) (Fig.5).

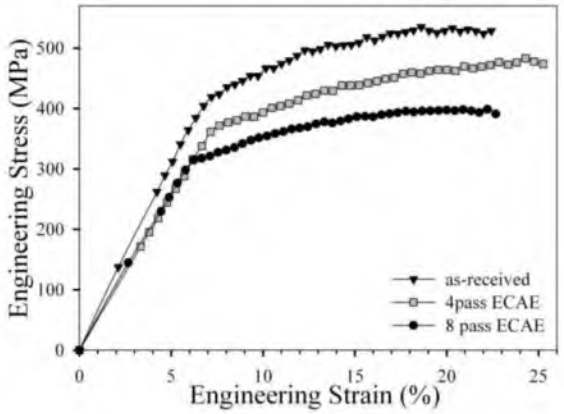


Fig. 5. The engineering stress-strain curves of the 1421 Al alloy at room temperature after the T6 heat-treatment.

**Discussion**

Thus, the fully recrystallized UFG structure evolved in the 1421 Al under ECAE remains essentially unchanged under solution treatment due to $Al_3(Sc,Zr)$ dispersoids which play a role of effective pinning agents hindering migration of HAGBs. Therefore, the 1421 Al can be subjected to precipitation-hardening without loss of UFG structure. However, UFG structure strongly effect the precipitation sequence under ageing. The normal precipitation sequence in Al-Li-Mg alloys during ageing is indicated by [2]:

$SSSS \rightarrow \delta'\ (Al_3Li) \rightarrow S_1(Al_2LiMg)$ (2).

It is known that $\delta'$ – phase is the main agent of precipitation hardening in Al-Li-Mg alloys [2]. The $S_1$-phase could not provide remarkable precipitation hardening due to its large size and location at triple junction and along HAGBs. In addition, Mg, which provides solid solution strengthening originated from the elastic distortions produced by substitutional Mg atom in the Al-Li matrix [2],

leaves solid solution for the formation of the $S_1$-phase. In the extruded material, the artificial ageing provides uniform precipitation of the δ' – phase dispersoids within grain interiors and high yield strength. In the 1421 Al with UFG structure the $S_1$-phase precipitates along grain boundaries under ageing condition; δ' – phase dissolves within grain interiors, concurrently. Lacking precipitation strengthening associated with uniform distribution of nanoscale δ' – phase could not be compensated by superposition of grain refinement strengthening and even additional dislocation strengthening associated with increased lattice dislocation density in the ECAE processed 1421 Al in comparison with the extruded material. This is why the strength of the ECAE processed 1421 Al is less than the strength of the same material in as-extruded condition. The difference in strength between samples subjected to ECAE with $\varepsilon \sim 4$ and $\varepsilon \sim 8$ is also associated with difference in phase composition. The presence of δ' – phase dispersoid in the 1421 Al subjected to ECAE with $\varepsilon \sim 4$ followed by T6 heat treatment provides increased strength in comparison with the 1421 Al subjected to subjected to ECAE with $\varepsilon \sim 8$. Thus, in order to achieve an increase in the strength of the 1421 Al by extensive grain refinement through ECAE the final heat treatment has to provide uniform precipitations of the δ' – phase within material body.

## References


[1] I.N. Fridlyander: Met.Sci.Heat Treat. no.1 (2001), p. 5.

[2] I.N. Fridlyander, K.V. Chuistova, A.L. Berezina, N.I. Kolobnev: *Aluminum - Lithium alloys. Structure and Properties* (Naukova Dumka, Kiev, 1992).

[3] R.Kaibyshev, K.Shipilova, F.Musin, Y.Motohashi: Mater.Sci.Techn., Vol. 21 (2005), p. 408.

[4] F. Musin, R.Kaibyshev, Y. Motohashi, T. Sakuma and G.Itoh: Mater.Trans. Vol. 43 (2002), p. 2370.

[5] S. Lee, P. B. Berbon, M. Furukawa, Z. Horita, M. Nemoto, N. K. Tsenev, R. Z. Valiev and T. G. Langdon: Mater. Sci .Eng., A272 (1999), p. 63.

[6] A.A. Mogucheva and R. O. Kaibyshev: Phys.Met.Metall. Vol. 106 (2008), p. 424.

[7] Z.C. Wang, P.B. Prangnell: Mater.Sci.Eng. A328 (2002), p. 87.

[8] H.G. Salem, R.E. Goforth, and K.T. Hartwig: Metall.Mater.Trans. Vol. 34A (2003), p. 153.

[9] R. Z.Valiev, T. G. Langdon, Prog.Mater.sci.: Vol. 51 (2006), p. 881.

[10]M. Kamachi, M. Furukawa, Z. Horita, T.G. Langdon: Mater. Sci. Eng.A. 361 (2003), p. 258.

[11]R.Kaibyshev, K.Shipilova, F.Musin, Y.Motohashi: Mater.Sci.Eng. Vol.396 (2005), p. 341.